An Investigation into the Correlations among GNSS Observations and their Impact on Height and Zenith Wet Delay Estimation for Medium and Long Baselines

Johnny Lo
School of Engineering, Edith Cowan University
Perth, WA, Australia
J.Lo@ecu.edu.au

Ahmed El-Mowafy
Department of Spatial Sciences, Curtin University
Perth, WA, Australia
A.El-mowafy@curtin.edu.au

ABSTRACT

Most stochastic modelling techniques neglect the correlations among the raw un-differenced observations when forming the variance-covariance matrix of the Global Navigation Satellite System (GNSS) observations. Some methods were developed to model these correlations. One such method is the Minimum Norm Quadratic Unbiased Estimator (MINQUE). Studies have shown that MINQUE improves ambiguity resolution, and ultimately, the positioning solution in short baselines. However, its effect in cases of processing with longer baselines and on the estimation of zenith wet delay (ZWD) is somewhat unknown. In this paper, a comparison between the impact of neglecting the correlations among the observations using an elevation-angle dependent model (EADM) and modelling the correlations using MINQUE on height determination and ZWD for medium and long baselines is carried out. The initial testing was carried out across two Australian GNSS stations with a medium-length baseline throughout a 3-week campaign. The results showed that using MINQUE did not resolve the coordinate and height components as accurate as the EADM. The results were further verified with two long-baseline campaigns whereby EADM was also able to provide better coordinate and wet delay estimates, and the inclusion of the correlations among the observations did not improve the results.

KEYWORDS: Stochastic models; MINQUE; ZWD; Heights

1 INTRODUCTION

GNSS data can be processed via the least-squares (LS) principle, in which, GNSS measurements are characterised by functional and stochastic models. The functional model represents the mathematical relationship among the GNSS observables and the parameters of interest, whilst the stochastic model is defined by an appropriate covariance matrix describing the spatial, auto, cross and/or temporal correlation among the measurements. The functional model, in its general form, is usually well defined (e.g., Hofmann-Wellenhof et al., 2001; Leick, 2004) and is not particularly controversial. On the other hand, stochastic modelling remains one of the more challenging aspects in precise GNSS positioning (e.g., Wang et al., 2002).

In LS theory, a set of linearised GNSS observations can be defined using the following functional regression model:

$$Y = A\hat{X} + \varepsilon \tag{1}$$

where for m observations and k unknowns, Y is an $m \times 1$ observations vector; $\hat{X}$ is a $k \times 1$ vector of estimates for the unknown parameters with A being the corresponding $m \times k$ design matrix; ε is an $m \times 1$ noise vector, with $E(\varepsilon) = 0$.

The simple form for the weighted linear LS estimate $\hat{X}$, is given by (Johnson and Wichern, 2007):

$$\hat{X} = (A^T W A)^{-1} A^T W Y \tag{2}$$

The covariance matrix of $\hat{X}$ is:

$$C_{\hat{X}} = (A^T W A)^{-1} \tag{3}$$

the weight matrix W is usually defined as the inverse of the variance-covariance matrix of the observations. From Eq. (2), it can be seen that the choice of stochastic model is an important factor in determining the final outcome of the LS parameter solution. LS possesses an attractive property in which the residual root mean square error (RMSE) is minimised. However, an inadequately defined covariance matrix will result in LS losing its optimality property (Johnson and Wichern, 2007). In real-time kinematic (RTK) data processing, where results are needed almost instantaneously, a wrongly chosen stochastic model may result in a faulty cycle slip detection and degraded ambiguity resolution success. The quality of the parameter estimates of interest, such as receiver coordinates, will accordingly suffer as a result (Fuller et al., 2005).

Typically the correlations among the raw measurements are ignored and the covariance matrix is estimated using an elevation-angle-dependent model (e.g., Kim and Langley, 2001) or the signal-to-noise ratio model (e.g., Ward, 1996). The elevation-angle-dependent model (EADM), has been shown to produce reliable tropospheric estimates (e.g., Steigenberger et al., 2007). Although more rigorous stochastic modelling techniques are available, (e.g., Wang et al., 1998; Teunissen and Amiri-Simkooei, 2007), the complexity of these models generally demands more processing time. Additionally, these models have predominantly been used to derive positional and integer ambiguity estimates, and the effects on tropospheric estimates are still relatively unknown. Though one may hypothesise that better coordinates would lead to better tropospheric delay estimation, the significance of this is still speculative.

The above issue leads to the objective of this investigation, which is to determine if the estimation of tropospheric delay will benefit from a more sophisticated stochastic model that considers possible spatial correlations among observations. A suggested model is the Minimum Norm Quadratic Unbiased Estimation 'MINQUE' (Rao, 1970). MINQUE had been successfully applied in GNSS data processing, where it was shown to improve short baseline solutions, as well as ambiguity resolution (Wang et al., 1998). However, it has not yet been used for the purpose of tropospheric delay recovery, which is needed for real-time precise positioning and weather forecast applications. In this paper, the performance of MINQUE for both tropospheric delay and height estimation, where the accuracy of the tropospheric estimates is related to the estimation of the height component are compared against a widely-

used stochastic model, i.e., EADM. A simplified form of MINQUE (Satirapod et al., 2002) is also tested.

The structure for the rest of this paper is as follows. Section 2 provides detailed description of the stochastic models under consideration. Testing of the stochastic models begins with a medium-length baseline campaign in the state of Victoria. The test description and results are presented in Section 3. The investigation next includes two long-baseline campaigns. Details of the campaigns are outlined in Section 4, along with the test results. Concluding remarks and recommendations are given in Section 5.

2 STOCHASTIC MODELS

In this section, three stochastic models are presented. The first, EADM, neglects the correlations among the raw observations and the second, MINQUE, models such correlations. The third model, SMINQUE, is a simplified version of MINQUE that can also estimate the correlation values.

2.1 Elevation Angle Dependent Model (EADM)

The dependence of measurement noise on satellite elevation can be attributed to changes that take place in the receiver antenna's gain pattern, atmospheric refraction and multipath with changes in the satellite elevation-angle (e.g., Kim and Langley 2001, El-Mowafy 2009). Modelling the observational noise as a function of the satellite elevation angle can take on many forms. The variance in one of these elevation angle-based models for observation y_i has the general form (Wang et al., 1998):

$$\sigma_{y_i}^2 = a^2 + b^2 f\left(\theta_z^i\right) \tag{4}$$

where a^2 and b^2 are constant coefficients and $f\left(\theta_z^i\right)$ is the function that is defined with respect to the zenith elevation angle θ_z^i for observation i. The sine function can be utilized to define the variances of the zero difference measurements in the form (Jin et al., 2005):

$$\sigma_{y_i}^2 = a^2 + b^2 \sin^2\left(\theta_z^i\right) \tag{5}$$

neglecting the case where the elevation angle equals 0^o (which is acceptable as measurements are usually ignored at low angles). The EADM de-weights the observations at low elevation angles which are more susceptible to multipath and troposphere errors. For the purpose of simplicity, the coefficients a and b can be chosen as 0 and 1. The raw observations in the EADM are assumed to be spatially and temporally uncorrelated. Thus, the undifferenced covariance matrix is taken as a diagonal matrix. The attraction of EADM is its practicality in term of computational efficiency.

2.2 Minimum Norm Quadratic Unbiased Estimation (MINQUE)

MINQUE is a stochastic technique that estimates the spatial correlations among the GNSS observations. However, the complexity of the MINQUE procedure comes from the need to utilise it in a batch processing. Hence, MINQUE is more appropriate in post-processing.

Using the functional model given in Eq. (1), the $m \times m$ covariance matrix of Y, denoted as Σ, can be expressed as follows:

$$\Sigma = \sum_{i=1}^{q} C_i = \sum_{i=1}^{q} \phi_i V_i , \qquad \text{where } q = \frac{m(m+1)}{2} \tag{6}$$

$\{\phi_1, \phi_2, ..., \phi_q\} = \{\sigma_1^2, \sigma_2^2, ..., \sigma_m^2, \sigma_{12}, \sigma_{13}, ..., \sigma_{m(m-1)}\}$ are the covariance components to be estimated, and $V_1, V_2, ..., V_q$ are the so-called accompanying matrices (Wang et al., 2002). The problem here is estimating the q unknown elements of ϕ and V.

The MINQUE of the linear function ϕ_i (for $i = 1, 2, ..., q$), i.e., $p_1\phi_1 + p_2\phi_2 + ... + p_q\phi_q$, is the quadratic function $Y^T BY$, where B is selected such that Trace(BΣBΣ) is minimum (Rao , 1971), subject to

$$BA = 0 \text{ and } \text{Trace}(BC_i) = p_i, \quad i = 1, 2, ..., q \tag{7}$$

The MINQUE of $\sum_{i=1}^{q} \phi_i V_i$ is then estimated from

$$\gamma^T Q = \sum_{i=1}^{q} \gamma_i Q_i , \qquad \text{where } Q_i = Y^T R V_i R Y \tag{8}$$

where the vector γ is a solution of

$$\sum_{i=1}^{q} \gamma_i \text{Trace}(RV_i RV_j) = p_j, \text{ for } j = 1, 2, ..., q \tag{9}$$

and

$$R = W (W^{-1} - X (X^T W X)^{-1} X^T) W, \tag{10}$$

where

$$W = \Sigma^{-1} \text{ (inverse of the covariance matrix } \Sigma \text{ of the observations)} \tag{11}$$

For n number of epochs considered in a selected processing window, the symmetric matrix R can be partitioned as

$$R = \begin{bmatrix} R_{11} & R_{12} & \cdots & R_{1n} \\ R_{21} & R_{22} & \ddots & R_{2n} \\ \vdots & \ddots & \ddots & \vdots \\ R_{n1} & R_{n2} & ... & R_{nn} \end{bmatrix} \tag{12}$$

By expressing Eq. (9) as $S\gamma = p$, and defining the elements of the S matrix, S_{ij}, as

$$S_{ij} = \text{Trace}(RV_i RV_j) \tag{13}$$

this leads to $\gamma = S^{-1}p$.

Since the MINQUE of $\sum_{i=1}^{q}\phi_i V_i$ is

$$\gamma^T Q = p^T \left(S^{-1}\right)^T Q = p^T S^{-1} Q = p^T \hat{\phi} \tag{14}$$

then $\hat{\phi} = \left(\hat{\phi}_1, \hat{\phi}_2, ..., \hat{\phi}_q\right)$ is a solution of

$$\hat{S}\phi = \hat{Q} \tag{15}$$

$\hat{Q}$ can alternatively be defined as

$$\hat{Q}_i = Y^T R V_i R Y = \varepsilon^T W V_i \varepsilon \tag{16}$$

Given an initial estimate $\hat{\phi}_{(0)}$, the $(j+1)^{th}$ approximation can be generated using the following iterative procedure

$$\hat{\phi}_{(j+1)} = S_{(j)}^{-1}\, \hat{Q}_{(j+1)}, \quad \text{for } j = 0, 1, 2, \ldots \tag{17}$$

2.3 Simplified MINQUE (SMINQUE)

As the number of observations becomes large, the execution of MINQUE will require a substantial computational power and memory. This is mostly due to the computation and storage of the R matrix, given in Eq. (12). The notion behind the simplified MINQUE (Satirapod et al., 2002), which will be referred to here as SMINQUE, is to reduce the complexity of the R matrix, leading to the efficient computation of the MINQUE process. The proposed simplification of MINQUE disregards the off-diagonal block entries of the R matrix and considers a block-diagonal matrix R* as its replacement in the procedure. The R* matrix is expressed as:

$$R^* = \begin{bmatrix} R_{11} & 0 & \cdots & 0 \\ 0 & R_{22} & \ddots & \vdots \\ \vdots & \ddots & \ddots & 0 \\ 0 & \cdots & 0 & R_{nn} \end{bmatrix} \tag{18}$$

Subsequently, Eq. (13) can be simplified to

$$S_{ij} = \sum_{r=1}^{n} \text{Trace}\left(R_{rr} V_{ir} R_{rr} V_{jr}\right) \tag{19}$$

where V_{ir} is the block-diagonal element of V_i for epoch r.

3 TESTING OF DIFFERENT STOCHASTIC MODELS FOR MEDIUM BASELINE

3.1 Test Description

The purpose of this manuscript is to determine whether the inclusion of spatial correlations in the stochastic model using MINQUE can improve the coordinate and tropospheric solutions over medium to long baselines. Up until now, MINQUE has only been used for relatively small processing windows, and over relatively short baselines (<15km) due to its computational demands (e.g., Wang et al., 1998; Satirapod et al., 2002; Wang et al., 2002). These studies were also carried out over short isolated periods. A study of the stations coordinates over a prolonged time period, as a result of using MINQUE, is also lacking. The usefulness of MINQUE over longer baselines has not yet been investigated. Furthermore, its impact on the estimation of tropospheric delays is still unknown. However, the accuracy of the tropospheric estimates is related to the estimation of the height component (Bock et al., 2001). Therefore, it is important to understand the impact of MINQUE on the height component firstly over a medium-length baseline before proceeding to a long-scale baseline or a network campaign. For this purpose, a medium-length baseline was set up between two Australian stations, namely Ballarat (BALL) and Melbourne Observatory (MOBS) in the state of Victoria (see Figure 1).

Figure 1 Locations of Ballarat and Melbourne Observatory test stations

MOBS is an International GNSS Service (IGS) station from the Australian Regional GPS (Global Positioning System) network, and BALL is a station from the Australian Continuously Operating Reference Station (CORS) network. For this baseline campaign, three weeks of data from March 31st to April 22th in 2004 were selected for post processing. The ITRF (x, y, z) Cartesian coordinates for MOBS and BALL for the testing period is (–4130636.1116, 2894953.1117, –3890531.0333) and (–4088335.4061, 2986195.6103, –3867029.3597), respectively. The medium baseline length between MOBS and BALL stations is approximately 103 km. MOBS uses an Ashtech UZ-12 receiver with a ASH701945C_M antenna, whilst BALL utilises a Trimble 4000SSI receiver and a Dorne Margolin T (with choke ring) antenna. Both test data in this study were dual frequency GPS data. The data were analysed with 1 h, 2 h, 3 h and 6 h processing windows. In other words, the data were batch-processed at every 1 h, 2h , 3 h or 6 h block throughout each day for the whole 3-week campaign.

To ensure that "absolute" tropospheric delays can be estimated appropriately a long baseline length is required (Kouba, 2009). Tregoning (1998) also indicated that a baseline length of more than 2000 km is more appropriate in providing sufficient de-correlation of the observations between the two baseline stations to enable better absolute estimation of the zenith wet delay (ZWD). Therefore, due to the medium length of the MOBS-BALL baseline, estimation of the absolute tropospheric delay at the stations was not appropriate. A longer baseline was examined, which will be discussed in the next section.

All data were processed with the Bernese GPS software package (Dach et al., 2007). IGS products concerning the monitoring stations, including precise satellite ephemerides, Earth Orientation Parameters (EOPs), coordinates and velocity of ground stations, antenna phase centre offsets and variations were used in the processing. During processing, the station coordinates; satellite and receiver clock offsets and the tropospheric zenith delay were estimated as the unknown parameters. The processing included the use of a cut-off elevation angle of 15^0 and the Niell troposphere mapping functions. The ionosphere-free linear combination was implemented to mitigate the ionospheric residual errors.

In the MOBS-BALL baseline campaign, the coordinates of MOBS were constrained to within 0.1 mm from the International Terrestrial Reference Frame 2008 (ITRF2008) estimates on the 31st of March 2004. The impact of MINQUE and SMINQUE were realised from the estimated coordinate solutions of BALL, since the coordinates for BALL were known beforehand. Thus, accuracy of the Cartesian and height coordinates for BALL, estimated independently using the EADM, MINQUE and SMINQUE were assessed by comparing the estimated values with the known ITRF2008 values.

3.2 TEST RESULTS OF THE MOBS-BALL BASELINE

The accuracy, i.e. the root mean square error (RMSE) of each of the x, y, z and h coordinates obtained from each of the tested stochastic models, namely EADM, MINQUE and SMINQUE, are calculated using

$$\mathrm{RMSE} = \sqrt{\sum_{i=1}^{k} \frac{(\Delta \mathrm{Coordinate}_i)^2}{k}} \tag{20}$$

where $\Delta\mathrm{Coordinate} = \Delta x$, Δy, Δz or Δh and k is the total number of coordinate solutions over the 3-week testing period.

The RMSE results are summarised in Figure 2. The top-left, top-right, bottom left and bottom right diagrams represent the results for when the data were analysed with a 1 h, 2 h, 3 h and 6 h processing window session. The RMSE of the coordinate and height discrepancies (offsets), indicated as bars in Figure 2, were determined from all solutions over the whole 3-week campaign.

It is evident from Figure 2 that the EADM consistently produced the best results among the three presented stochastic models with respect to the RMSE of the Cartesian and height discrepancies. Although studies have shown that MINQUE and MINQUE can produce better coordinate solutions for short baselines of less than 15 km (e.g., Wang et al., 1998; Satirapod et al., 2002; Wang et al., 2002), this improvement was not evident over a longer baseline, as shown by the MOBS-BALL baseline campaign. An increase in the baseline length generally leads to an increase in the residual errors due to differences in the troposphere, ionosphere,

and other location-dependent factors experienced at each respective station (e.g., Eckl et al., 2001). The EADM is location sensitive as it weighs the raw GNSS observations by considering the elevation angles from different satellites to a particular location. The greater the elevation angle, the more atmosphere GNSS signal pass through and hence, larger residual errors. However, MINQUE and SMINQUE do not consider these factors in their modelling the correlations. This is a possible explanation as to why they were outperformed by EADM.

As stated earlier, the aforementioned studies on MINQUE were never used for an extended period of time for a baseline campaign. Although there were instances whereby the MINQUE produced better coordinates than the EADM, the 3-week campaign outlined in this study revealed that the results by MINQUE and SMINQUE have poor repeatability overall.

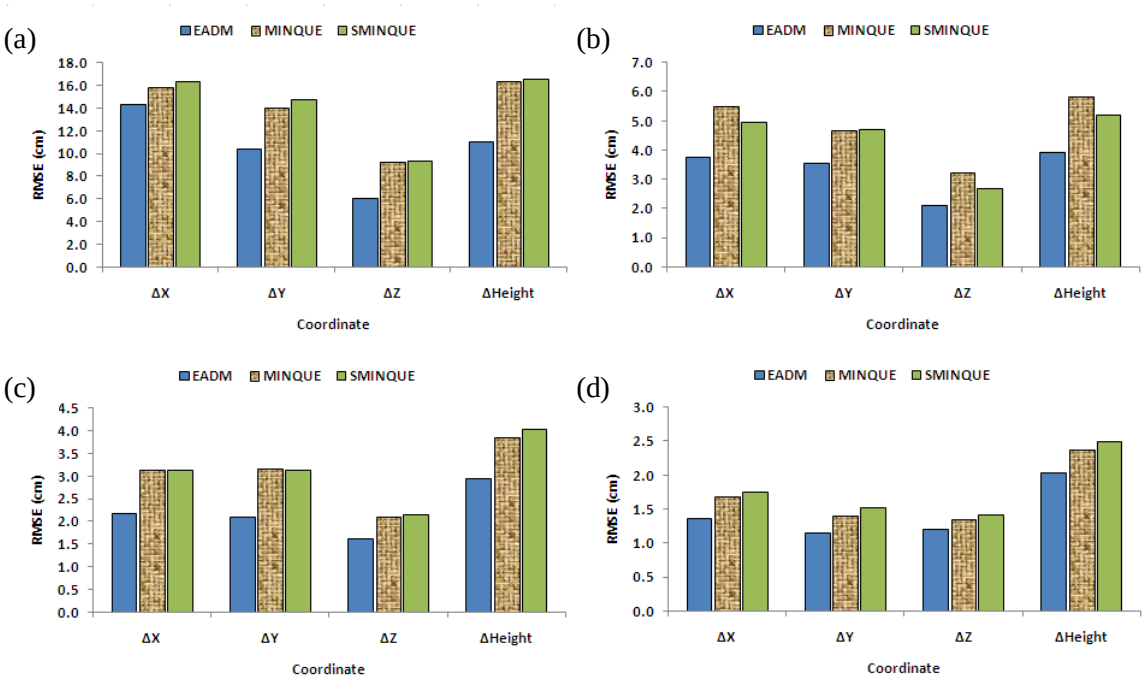

Figure 2 Plots of the Cartesian and height coordinate discrepancies at BALL for the MOBS-BALL baseline campaign for (a)1 h, (b) 2 h, (c) 3 h and (d) 6 h of processing.

4 TESTING OF DIFFERENT STOCHASTIC MODELS FOR LONG BASELINE

4.1 Test Description

As it is necessary to have a much longer baseline to obtain absolute tropospheric estimates, a long-baseline campaign in Australia (Alice Springs to Hobart (ALIC-HOB2)) and one in Europe (Onsala to Wettzell (ONSA-WTZR)) were set up and analysed. Locations of the stations are presented in Figure 3.

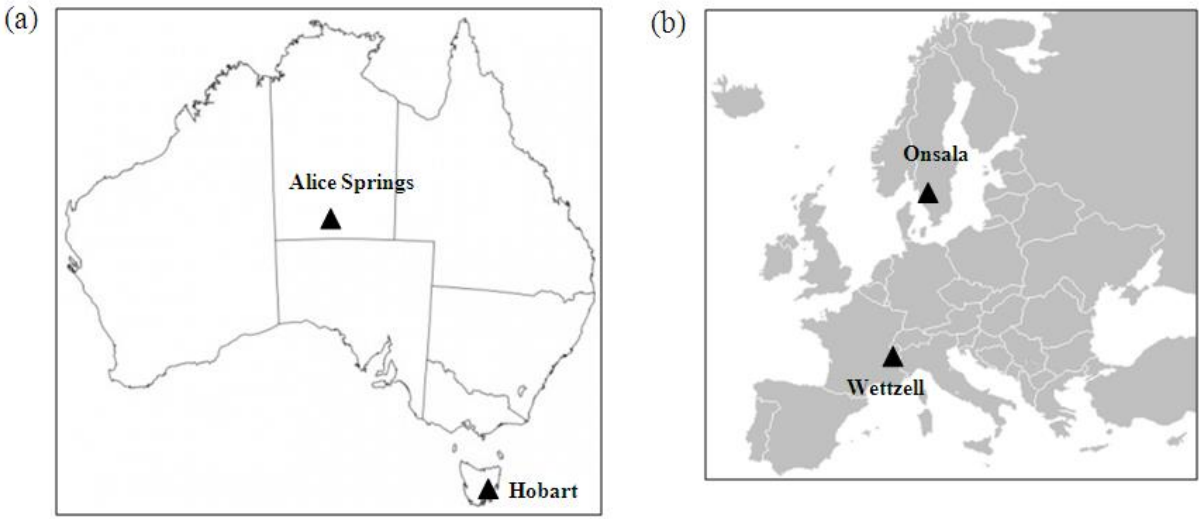

Figure 3 Locations of (a) Alice Spring and Hobart GNSS stations in Australia, and (b) Wettzell and Onsala station in Europe.

A week of data from March 31st to April 6th in 2004 was selected for the Australian baseline campaign, whilst two weeks of data from September 10th to 23rd in 2003 were used for the European campaign. The selected periods correspond to the autumn season in the respective region. This season has high diurnal variation and thus, allowing the stochastic models to demonstrate their capability under varying atmospheric conditions. All stations in the ALIC-HOB2 and ONSA-WTZR baseline campaigns are IGS stations, and hence their coordinates are known with a high degree of accuracy (Kouba, 2009). The (*x*, *y*, *z*) Cartesian coordinates of the stations for the testing period are given in Table 1. The lengths of the baselines are approximately 2447 km and 920 km respectively, which ensured that the absolute zenith tropospheric delays can be estimated from the campaigns along with the coordinates.

Table 1 Cartesian coordinates for the Australian and European stations

Station	ITRF2008 Coordinates		
	x	y	z
ALIC	–4052052.1042	4212836.1056	–2545105.5242
HOB2	–3950071.6113	2522415.2415	–4311638.1117
ONSA	3370658.5630	711877.1203	5349786.9403
WTZR	4075580.5771	931853.7760	4801568.1232

The receiver and antenna models for each station are outlined in Table 2. Products concerning the antenna phase offsets were used in the process to mitigate subsequent residual errors.

Table 2 Receiver and antenna model for the Australian and European stations

Station	Receiver Model	Antenna Model
ALIC	AOA ICS-4000Z AC	AOAD/M_T
HOB2	AOA ICS-4000Z AC	AOAD/M_T
ONSA	ROGUE SNR-8000	AOAD/M_B
WTZR	ROGUE SNR-8000	AOAD/M_T

Other IGS products such as precise ephemerides, ocean tide loadings and EOPs were also used in post-processing. The processing parameters were the same as the MOBS-BALL campaign, i.e. the station coordinates; satellite and receiver clock offsets and the tropospheric zenith delay were estimated as the unknown parameters. The processing included the use of a cut-off elevation angle of 15^0 and the Niell troposphere mapping functions. The ionosphere-free linear combination was implemented to mitigate the ionospheric residual errors. The data were analysed with 1 h, 2 h, and 3 h processing windows. The tropospheric parameter was estimated at every hour, regardless of the size of the processing session. The ALIC and ONSA stations were chosen as the reference station in each respective campaign and their coordinates were constrained to within 0.1 mm from the ITRF2008 coordinates. The accuracy of the Cartesian and height coordinates of HOB2 and WTZR, estimated independently using EADM, MINQUE and SMINQUE were assessed by comparing the estimated values with the known ITRF2008 coordinates. For the ALIC-HOB2 campaign, the ITRF coordinates were calculated on the 31st of March2004, whereas for the ONSA-WTZR campaign the coordinates for the stations were calculated on the 10th of September 2004. The corresponding hourly GNSS precipitable water vapour (PWV) estimates for the ALIC-HOB2 campaign were converted from the ZWD estimates using the following equations (e.g. Bevis et al., 1992):

$$\mathrm{PWV} = \Pi \times \mathrm{ZWD} \tag{21}$$

with

$$\Pi = 10^6 \rho_w R_{wv} \left(k_2' + \frac{k_3}{T_m} \right) \tag{22}$$

and

$$k_2^{'} = k_2 - k_1 \frac{M_{wv}}{M_d} \tag{23}$$

$$T_m = 70.2 + 0.72 T_s \tag{24}$$

where R_{wv} and ρ_w are the specific gas constant of water vapour and the density of liquid water, respectively; T_m is the weighted mean temperature; T_s is the surface temperature in Kelvin; M_{wv} and M_d are the molecular mass of water vapour and dry air, respectively; k_1, k_2, k_3 are the pre-determined coefficients based on theory and experimental observations. Table 3 provides the values for these coefficients.

Table 3 Values for Coefficients k_1, k_2 and k_3

	k_1(Kmbar^{-1})	k_2(Kmbar^{-1})	k_3(K^{2}mbar^{-1})
Smith and Weintraub (1953)	77.607 ± 0.013	71.60 ± 8.50	3.747 ± 0.031
Thayer (1974)	77.604 ± 0.014	64.79 ± 0.08	3.776 ± 0.004
Bevis *et al.*(1994)	77.600 ± 0.050	70.40 ± 2.20	3.739 ± 0.012

The factor Π is sometimes approximated as 6.5 (Kleijer, 2004), but it varies spatially and temporally.

Once estimated, the PWV were then validated against co-located radiosonde (RS) data. The RS data were provided by the Australian Bureau of Meteorology (BoM) twice daily at 0:00 and 12:00 Coordinated Universal Time (UTC), together with other relevant surface meteorological data such as temperature and pressure data. The meteorological data allow the GNSS wet delay estimates to be converted to PWV estimates using eqs. (21) – (24).

Unfortunately, RS data were not available for the ONSA-WTZR baseline campaign; however, water vapour radiometer (WVR) data were accessible for comparisons. A WVR is able to direct measure the amount of water vapour (i.e. wet delay) in the atmosphere along a line-of-sight. The WVR data at ONSA were available at every 60 seconds whilst hourly WVR data were provided at WTZR. However, the WVR data Onsala were averaged at every hour to ensure that comparisons can be made with the hourly GNSS ZWD estimates.

4.2 TEST RESULTS OF THE ALIC-HOB2 AND ONSA-WTZR BASELINES

The RMSE, calculated using eq. (20), for each of the tested stochastic models, namely EADM, MINQUE and SMINQUE, are summarised in Figure 4 and Figure 5 for HOB2 and WTZR stations, respectively. The given RMSE of the coordinate and height discrepancies (offsets) were determined from all solutions over the whole investigated period of the campaigns. In each of these figures, the top-left, top-right and bottom diagrams represent the results for when the data were analysed with 1 h, 2 h and 3 h processing windows.

The magnitude of the RMSE for these small processing windows can be attributed to the large baseline length, i.e. greater residual errors. As expected, the coordinate solutions improve with increasing processing window size. For the ALIC-HOB2 campaign, the EADM consistently produced the best results among the three presented stochastic models with respect to the accuracy of the coordinate offsets from the referenced ITRF values. The MINQUE method did perform marginally better with the 2 h processing window than the EADM. The differences between the MINQUE and SMINQUE were generally in the sub-millimetre range. However, differences of up to a few millimetres were also observed.

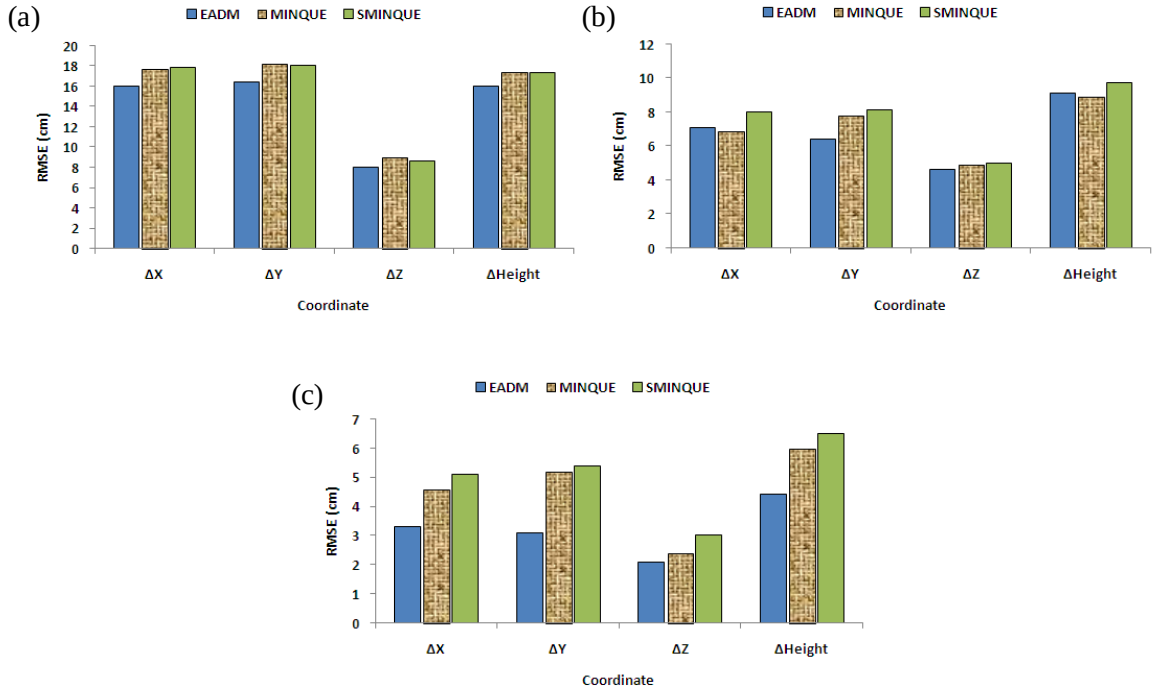

Figure 4 Plots of the Cartesian and height coordinate discrepancies at HOB2 for the ALIC-HOB2 baseline campaign for (a) 1 h, (b) 2 h and (c) 3 h processing windows

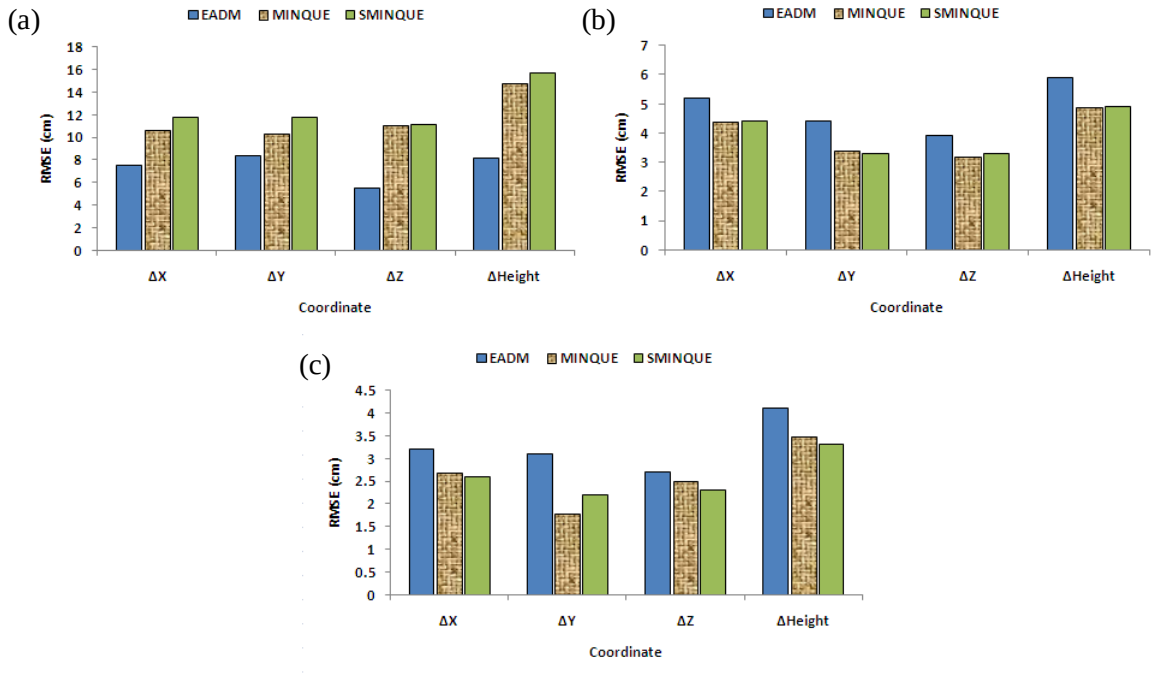

Figure 5 Plots of the Cartesian and height coordinate discrepancies at WTZR for the ONSA-WTZR baseline campaign (a) 1 h, (b) 2 h and (c) 3 h processing windows

The positional results, shown in Figure 5, for the ONSA-WTZR baseline with a 1 h processing window were similar to that of the ALIC-HOB2 baseline in that the MINQUE and SMINQUE models performed relatively poorly in comparison to that of EADM. However, the MINQUE and SMINQUE models showed improvements for the 2 h and 3 h windows. In fact, the MINQUE and SMINQUE models produced better coordinate solutions. The more favourable results from the ONSA-WTZR campaign (as compared to ALIC-HOB2) can be attributed to smaller location-dependent residual errors due to shorter baseline length, as well as a smaller difference in latitudes between the two stations and thus, both stations experienced somewhat similar satellite geometry and atmospheric effects.

The RMSE is used to evaluate the accuracy of corresponding set of GNSS tropospheric solutions for these campaigns. The RMSE for the differences between GNSS and RS PWV and for the differences between GNSS and WVR ZWD estimates is computed as follows:

$$\mathrm{RMSE} = \sqrt{\frac{\sum_{j=1}^{n_c}\left(\mathrm{PWV}_{\mathrm{GNSS}}^{(j)} - \mathrm{PWV}_{\mathrm{RS}}^{(j)}\right)^2}{n_c}} \quad \text{or} \quad \mathrm{RMSE} = \sqrt{\frac{\sum_{j=1}^{n_c}\left(\mathrm{ZWD}_{\mathrm{GNSS}}^{(j)} - \mathrm{ZWD}_{\mathrm{WVR}}^{(j)}\right)^2}{n_c}} \qquad (25)$$

where n_c refers to the number of data compared.

The RMSE of the PWV differences for ALIC and HOB2 are summarised in the Tables 4 and 5, which showed that the EADM was superior to the MINQUE and SMINQUE models in resolving the PWV estimates, in additional to providing better positional estimates (as shown in Figure 4). On average, the EADM was able to provide PWV estimates with an improvement of approximately 38 % and 45 % in accuracy when compared to the PWV values estimated from the MINQUE and SMINQUE models. Although it was not as prominent at HOB2, an improvement in the resolution of the PWV estimates can be observed nonetheless.

Table 4 RMSE (mm) of the PWV differences between GNSS and RS measurements at Alice Springs

Window Size	EADM	MINQUE	SMINQUE
1 h	3.2	5.8	5.6
2 h	2.2	3.0	4.1
3 h	1.1	1.6	2.2

Table 5 RMSE (mm) of the PWV differences between GNSS and RS measurements at Hobart

Window Size	EADM	MINQUE	SMINQUE
1 h	2.3	3.7	2.2
2 h	1.6	2.0	2.0
3 h	2.2	2.4	2.2

For the European campaign, the RMSE of the ZWD differences between the GNSS and WVR estimates for ONSA and WTZR are summarised in the Tables 6 and 7. For the ONSA-WTZR baseline campaign, the EADM outperformed the other stochastic models with the 1 h processing window as a result of better height estimates. Although the MINQUE and SMINQUE models yielded slightly better positional estimates for the 2 h and 3 h processing windows, this improvement was not evident in the subsequent ZWD estimates.

Table 6 RMSE (cm) of the ZWD differences between GNSS and WVR measurements at Onsala

Window Size	EADM	MINQUE	SMINQUE
1 h	2.4	2.8	2.8
2 h	1.7	1.8	1.8
3 h	1.4	1.7	1.7

Table 7 RMSE (cm) of the ZWD differences between GNSS and WVR measurements at Wettzell

Window Size	EADM	MINQUE	SMINQUE
1 h	3.0	3.2	3.5
2 h	2.1	2.3	2.2
3 h	1.9	2.0	2.0

In fact, the EADM was the top-performer across all processing window sizes. On average, the EADM was able to resolve the ZWD with a 12.5% improvement in RMSE over MINQUE and SMINQUE at the Onsala stations. The advantage of using EADM was also evident at WTZR with the average improvements in RMSE of around 7% and 8% over MINQUE and SMINQUE.

The favourable results for EADM in these campaigns can be attributed to the fact that the weights given by the model reflect the amount atmosphere experienced by GNSS signals. Furthermore, the EADM is a model that provides greater weights to the observations closer to the zenith, and de-weights observations at lower elevation angles and hence, reduces troposphere errors. In contrast, MINQUE is a model that only considers the spatial correlations among the satellites and it does not take into account location-dependent errors due to the troposphere. From results of the investigations in this paper, the use of EADM is therefore recommended for the purpose of estimating tropospheric delays.

Although the EADM is a conventional model that ignores any correlations among the undifferenced observations, it was shown in this study to be superior to MINQUE and SMINQUE, models that consider the spatial correlation among the GNSS observations in estimating the tropospheric delays. The computational power required by MINQUE is also a hindrance. Further studies are planned to determine if the results here are reflective of other spatial models such as Maximum Likelihood Estimator, Best Invariant Quadratic Unbiased Estimator and Lehmann-Scheffé Estimator (Amiri-Simkooei, 2007; Slanger, 1996).

5 SUMMARY

Changes in the stochastic model to include the correlations among the GNSS observations affect the estimation of heights and ZWD. In this paper, a study into the impact of MINQUE and SMINQUE over a medium length baseline of approximate length of 103 km was first presented. The baseline was processed with 1 h, a 2 h, a 3 h and a 6 h processing windows for a 3-week period. The results have shown that the MINQUE model was consistently outperformed by the EADM in resolving the Cartesian and height components by about 50% on average over the whole campaign.

For the investigation of a long-baseline campaign in Australia, MINQUE and SMINQUE models were again outperformed by EADM. The accuracy of the corresponding tropospheric solutions suffers as a consequence and it was found that the EADM was able to resolve the PWV solutions on average 40% more accurately. Although the positional results for EADM in another baseline campaign between Onsala and Wettzell were mixed, it managed to provide the better set of tropospheric solutions in terms of smaller RMSE values. Overall, the study shows that the modelling of the correlation is not as significant in medium to long baselines. Thus, the use of EADM is recommended for the purpose of estimating positional solutions and tropospheric delays in these instances due to its simplicity.

ACKNOWLEDGEMENTS

This work was completed under a scholarship from Curtin University of Technology, Perth, Australia, and through Australian Research Council APAI grant LP0347723 in collaboration with the Australian Bureau of Meteorology. Special thanks to Prof. Gunanr Elgered, Mr Walter Schwarz and Land Victoria (www.landvic.gov.au) for providing the radiosonde and water vapour radiometer data. Discussions with Dr. Jinling Wang and Dr. Chalermchon Satirapod were valuable. Feedback on the manuscript from Dr. Nigel Penna is also much appreciated.

REFRENCES

Amiri_Simkooei, A. 2007. Least-squares variance component estimation: theory and GPS applications, PhD, Department of Mathematical Geodesy and Positioning, Delft University of Technology, Netherlands.

Bevis, M., S. Businger, T. A. Herring, C. Rocken, R. A. Anthes, and R. H. Ware. 1992. GPS meteorology: remote sensing of atmospheric water vapor using the global positioning system. *Journal of Geophysical Research* 97 (D14): 15787-15801.

Bevis, M., S. Businger, S. Chiswell, T. A. Herring, R. A. Anthes, C. Rocken, and R. H. Ware. 1994. GPS meteorology: mapping zenith wet delays onto precipitable water. *Journal of Applied Meteorology* 33 (3): 379-386.

Baker, H. C., A. H. Dodson, N. T. Penna, M. Higgins, and D. Offiler. 2001. Ground-based GPS water vapour estimation: potential for meteorological forecasting. *Journal of Atmospheric and Solar-Terrestrial Physics* 63 (12): 1305-1314.

Bock, O., J. Tarniewicz, C. Thom, J. Pelon, and M. Kasser. 2001. Study of external path delay correction techniques for high accuracy height determination with GNSS. *Physics and Chemistry of the Earth, Part A: Solid Earth and Geodesy* 26:165-171.

Dach, R., U. Hugentobler, P. Fridez, P. and M. Meindl, eds. 2007. *Bernese GPS software version 5.0*: Astronomical Institute University of Berne.

Eckl, M.C., R.A. Snay, T.Soler, M.W. Cline and G.L. Mader. 2001 Accuracy of GPS-derived relative positions as a function of interstation distance and observing -session duration. *Journal of Geodesy* 75(12):633-640.

El-Mowafy, A. 2009. An Alternative Post-Processing Relative Positioning Approach Based on Precise Point Positioning", *Journal of Surveying Engineering, ASCE*, 135(2): 56-65.

Fuller, S., P. Collier, and A. Kealy. 2005. Real time quality asseEWMent for CORS networks. *Journal of Global Positioning Systems* 4 (1-2):223-229.

Gutman, S. I., S. R. Sahm, S. G. Benjamin, B. E. Schwartz, K. L. Holub, J. Q. Stewart, and T. L. Smith. 2004. Rapid retrieval and assimilation of ground based GPS precipitable water observations at the NOAA forecast systems laboratory: Impact on weather forecasts. *Journal of the Meteorological Society of Japan* 82 (1B): 351-360.

Hofmann-Wellenhof, B., H. Lichtenegger, and J. Collins. 2001. *GNSS theory and practice*. 5th ed. New York: Springer-Verlag Wien, 382pp.

Jin, S., J. Wang, and P.H. Park. 2005. An improvement of GNSS height estimations: stochastic modeling. *Earth Planets Space* 57:253-259.

Johnson, R.A., and D.W. Wichern. 2007. *Applied multivariate statistical analysis*. 6th ed. London, UK: Prentice-Hall, 800pp.

Kim, D., and R.B. Langley. 2001. Quality control techniques and issues in GNSS applications: Stochastic modeling and reliability test. In *International Symposium on GNSS/GNSS (the 8th GNSS Workshop)*. Jeju Island, Japan.

King, R. W., and Y. Bock. 2002. *Documentation for the GAMIT GPS software version 4.2*. Cambridge, Massachusetts: Massachusetts Institute of Technology.

Kleijer, F. 2004. *Troposphere modeling and filtering for precise GPS leveling*. PhD, Department of Mathematical Geodesy and Positioning, Delft University of Technology, Netherlands.

Kouba, J. 2009. *A guide to using International GNSS Service (IGS) Products.* http://acc.igs.org/UsingIGSProductsVer21.pdf. (last accessed 16/5/12)

Leick, A. 2004. *GNSS Satellite Surveying*. 3rd ed. New Jersey, USA: John Wiley & Sons, Inc., 435pp.

Niell, A.E. 1996. Global mapping functions for the atmosphere delay at radio wavelenghts. *Journal of Geophysical Research* 101 (B2):3227-3246

Penna, N. T., J. Lo, and G. Luton. 2005. Geodetic GPS analysis of Land Victoria's GPSnet. *Journal of Spatial Science* 50 (1): 45-57.

Rao, C.R. 1970. Estimation of heterogeneous variances in linear models. *Journal of American Statistical Association* 65:161-172.

Rao, C.R., and J. Kleffe. 1988. *Estimation of variance components and applications*. Netherlands: Elsevier Science Publishers B.V., 361pp.

Saastamoinen, J. 1973. Contributions to the theory of atmospheric refraction. *Bullétin Géodésique* 105, 106, 107: 279-298, 383-397, 13-34.

Satirapod, C., J. Wang, and C. Rizos. 2002. A simplified MINQUE procedure for the estimation of variance-covariance components of GNSS observables. *Survey Review* 36 (286):582–590.

Schön, S., and H. Kutterer. 2006. Uncertainty in GPS networks due to remaining systematic errors: the interval approach. *Journal of Geodesy* 80 (3): 150-162.

Slanger, W.D. 1996. Least squares Lehmann-Scheffé estimation of variances and covariances with mixed linear models, *Journal of Animal Science*, 74:2577-2585.

Smith, E. K. and S. Weintraub. 1953. The constants in the equation for atmospheric refractive index at radio frequencies. *Proceedings of the Institute of Radio Engineers*. 41:1035-1037.

Steigenberger, P, V. Tesmer, M. Krügel, D. Thaller, R. Schmid, S. Vey, and M. Rothacher. 2007. Comparisons of homogeneously reprocessed GNSS and VLBI long time-series of troposphere zenith delays and gradients *Journal of Geodesy* 81 (6-8):503-514.

Teunissen, P.J.G., and A.R. Amiri-Simkooei. 2007. Least-squares variance component estimation *Journal of Geodesy* 82 (2):65-82, doi:10.1007/s00190-007-0157-x.

Thayer, G. D. 1974. An Improved equation for the Radio Refractive Index of Air, *Radio Science*, 9:803-807.

Tregoning, P., R. Boers, D. O'Brien, and M. Hendy. 1998. Accuracy of absolute precipitable water vapor estimates from GPS observations. *Journal of Geophysical Research* 103 (D22): 28,701-28,710.

Wang, J., C. Satirapod, and C. Rizos. 2002. Stochastic assessment of GNSS carrier phase measurements for precise static relative positioning. *Journal of Geodesy* 76 (2):95-104.

Wang, J., M.P. Stewart, and M Tsakiri. 1998. Stochastic modeling for static GNSS baseline data processing. *Journal of Surveying Engineering* 124 (4):171-181.

Wang, J., L. Zhang, A. Dai, T. van Hove, and J. van Baelen. 2007. A near-global, 2-hourly data set of atmospheric precipitable water from ground-based GPS measurements. *Journal of Geophysical Research* 112: D11107.

Ward, P. 1996. GPS Satellite Signal Characteristics. In *Understanding GPS Principles and Applications*, edited by Kaplan, E.D., 83-117. Artech House Publishers.